European Association for the Development of Renewable Energies, Environment and Power Quality

International Conference on Renewable Energies and Power Quality (ICREPQ'09)

Valencia (Spain), 15th to 17th April, 2009

Effects of flow direction and thermal short-circuiting on the performance of coaxial ground heat exchangers

E. Zanchini, S. Lazzari and A. Priarone

Dipartimento di Ingegneria Energetica, Nucleare e del Controllo Ambientale
Università di Bologna
Viale Risorgimento 2, I-40136, Bologna, Italia
Phone/Fax number:+39 051 2093295 / +39 051 2093296, e-mail: enzo.zanchini@unibo.it

Abstract. The effects of flow direction and thermal short-circuiting on the performance of coaxial ground heat exchangers are studied by finite-element simulations, performed through COMSOL Multiphysics 3.4 (©Comsol, Inc.). The real 2-D axisymmetric unsteady heat conduction and convection problem is considered. The distribution of the fluid bulk temperature in the inner circular tube is determined by means of the "weak boundary form" boundary condition available in COMSOL Multiphysics; the laminar convective heat transfer in the outer annular passage is simulated directly. Two Coaxial Ground Heat Exchangers (CGHEs) with the same length but different cross sections are examined; moreover, two values of the ground thermal conductivity, as well as two materials for the inner tube wall are considered. The results point out that the *annulus-in* flow direction (fluid inlet in the outer annular passage) is more efficient than the *center-in* flow direction (fluid inlet in the inner circular tube) and that the effect of short-circuiting is not very important, if the *annulus-in* flow direction is employed. Indeed, with this inlet configuration the energy loss for thermal short-circuiting is less than 1% for time intervals longer than 1 hour.

Key words

Ground Coupled Heat Pumps, Vertical Ground Heat Exchangers, Thermal Short-Circuiting, Flow Direction, Finite Element Simulations.

1. Introduction

Ground Coupled Heat Pumps (GCHPs) are based on heat transfer between the ground and a fluid, usually water, which circulates in tubes buried in the soil. Two different kinds of heat exchangers are employed: horizontal heat exchangers and vertical heat exchangers or Borehole Heat Exchangers (BHEs). BHEs have three different geometries:

1) single U-tube: only one U-bent polyethylene tube is placed in the borehole, which is then grouted;
2) double U-tube: two U-bent polyethylene tubes are placed in the borehole, which is then grouted;
3) two coaxial circular tubes, namely an internal polyethylene tube and an external tube, either inserted in a borehole (then grouted) or directly driven into the soil. The external tube is usually made of stainless steel; this choice is mandatory if the tube is driven into the soil.

The total length of a BHE necessary for a plant is usually determined by a method recommended by ASHRAE [1], which was proposed by Ingersoll and Zobel [2] and adjusted by Kavanaugh [3]. The final expressions for the total length require the knowledge of the effective thermal conductivity of the soil, k_g, of the effective thermal diffusivity of the soil, α_g, and of the borehole thermal resistance per unit length, R_b. The latter is determined mainly by the geometry of the borehole and by the thermal conductivity k_s of the grout (which is always present in U-tube BHEs). In order to determine k_g, α_g and R_b, a Thermal Response Test (TRT) is performed, according to the procedure prescribed by ASHRAE [1]. First, the undisturbed ground temperature T_g is determined, by one of the methods suggested in Ref. [4]. Then, by means of electric resistances, a constant power is supplied to the water which flows in the BHE and the following quantities are measured and recorded: the inlet fluid temperature T_{in}, the outlet fluid temperature T_{out}, the arithmetic mean fluid temperature $T_m = (T_{in} + T_{out})/2$, the mass flow rate $\dot{m}$ and the electric power $\dot{Q}_{el}$. The TRT has a minimum duration of 48 hours. The experimental data are processed by analytical or numerical methods to obtain best estimates of k_g, α_g and R_b.

The simplest method for the evaluation of a TRT is the analytical *line heat source* method, described, for instance, in Refs. [5, 6]. It considers the BHE as a linear power source within an infinite solid medium, which supplies to the medium a constant power per unit length

q_l. By employing an approximate form of the analytical solution for the temperature field $T(r, \tau)$, one obtains:

$$T_m(\tau) - T_g = \frac{q_l}{4\pi k_g} \ln \tau + C \quad , \tag{1}$$

where τ is time, starting from the beginning of the heating process, and C is a constant given by

$$C = q_l \left\{ R_b + \frac{1}{4\pi k_g} \left[\ln\left(\frac{4\alpha_g}{a^2} \right) - \gamma \right] \right\} \quad . \tag{2}$$

In Eq. (2), a is the borehole radius and $\gamma \approx 0.5772$ is Eulero constant.

Since the *line heat source* method does not take into account the heat capacity of the materials which form the BHE, Eqs. (1) and (2) are valid only if the time elapsed from the beginning of the heating process is greater than 15 hours. By means of a linear interpolation of the experimental values of $T_m(\tau) - T_g$ versus $\ln \tau$, one determines k_g and C. Then, one fixes a plausible value of α_g and determines R_b through Eq. (2). Clearly, the method contains heavy approximations; nevertheless, if correctly applied to sufficiently long TRTs, it yields acceptable values of k_g. The approximation on R_b is worse, also because it is affected by the uncertainty on the value assumed for α_g.

Most of the research on BHEs carried out in the last decade has concerned the development of methods which yield more precise values of α_g and R_b. For this purpose, numerical models for the evaluation of TRTs, as well as analytical and numerical studies of heat transfer mechanisms within BHEs have been developed.

In Ref. [7], a 2-D finite-volume numerical method for the simulation of unsteady heat transfer between a single U-tube BHE and the soil is presented. The method is validated by comparison with analytical models. In Ref. [8], the authors report the experimental results of some TRTs as well as the results of numerical evaluations of the TRTs, performed by the method proposed in Ref. [7]. The numerical evaluation has allowed the authors to determine the thermal conductivities k_g and k_s. In Ref. [9], four methods for the evaluation of TRTs are applied to the same data set and compared; in each case, the parameters k_g and R_b are evaluated. The methods are: two different applications of the *line heat source* method, a *cylindrical heat source* analytical method [9, 10], a 1-D finite-difference numerical method. The authors conclude that, while the *line heat source* method and the numerical method are in fair agreement with each other, the *cylindrical heat source* method overestimates the thermal conductivity of the ground and does not seem reliable.

In Ref. [4], two methods for measuring the undisturbed ground temperature are recommended: temperature logging along the borehole; circulating water through the borehole with electric resistances turned off and measuring the outlet fluid temperature at short time intervals until all the fluid contained in the borehole has come out.

Roth *et al.* [5] compare two methods for the evaluation of a TRT performed in Latin America: the analytical evaluation by the *line heat source* method and a 1-D numerical evaluation. In the numerical method, the borehole is sketched as the union of three domains: an internal water cylinder, a thin cylindrical layer without thermal inertia which represents the convective thermal resistance, a cylindrical layer which represents the grout.

In Ref. [11], the authors study the heat transfer within a BHE and exclude the ground. They consider steady-state conditions and assume that the temperature of the external surface of the BHE is uniform. They neglect the heat conduction in the vertical direction and, by employing some other approximations, they evaluate analytically the distribution of the fluid bulk temperature along the channels of a BHE. They consider both single U-tube and double U-tube BHEs. By employing the obtained temperature distributions, they evaluate the borehole thermal resistance as

$$R_b = \frac{T_m - T_w}{q_l} \quad , \tag{3}$$

where T_w is the temperature of the external surface of the BHE. The results point out that the thermal resistance of double U-tube BHEs is about 30% lower than that of single U-tube BHEs.

Lamarche and Beauchamp [12] propose a new analytical model for the evaluation of TRTs, valid also in the initial part of the heating process, and compare the analytical results with simulations obtained by means of COMSOL Multiphysics. The borehole is sketched as a water cylinder surrounded by a ring of grout, buried in the soil. Two thermal conditions are considered: uniform and constant heat flux at the internal surface of the grout; uniform water temperature and convective heat flux between water and grout. The paper refers to single U-tube BHEs; analytical results are in fair agreement with numerical simulations.

Marcotte and Pasquier [13] perform 3-D numerical simulations with COMSOL Multiphysics, with reference to a single U-tube BHE which absorbs a constant thermal power from the ground. They obtain the time evolution of the fluid bulk temperature distribution along the tubes. The results show that the true mean fluid temperature, T_f, does not coincide with the arithmetic mean fluid temperature, T_m, and that if T_m is employed instead of T_f to evaluate R_b by Eq. (3), then R_b is overestimated. The authors then propose a new expression of T_f for the evaluation of TRTs.

This short overview of relevant references reveals that most of the literature is devoted to the study of U-tube BHEs, which, indeed, are the most commonly used. Even for this geometry, the effect of thermal short-circuiting is seldom considered. In the quoted references, it is taken into account only in Refs. [11] and [13] and, even there, is not clearly evidenced. On the other hand, to account for thermal short-circuiting, a 4 to 6% increase in the effective thermal resistance of ground for a daily heat pulse is recommended by ASHRAE [1], in the use of the expressions for sizing U-tube BHEs piped in parallel.

The value of this increase parameter would deserve a deeper analysis. In addition, also vertical ground heat exchangers with coaxial tubes are now employed in Northern Italy, in the Padana Plain, where coaxial heat exchangers with an external stainless steel tube are directly driven into the soil, up to a depth of about 20 m. Since no bore is present in most applications of coaxial heat exchangers with the ground, they will be called Coaxial Ground Heat Exchangers (CGHEs). To our knowledge, no data are available in the literature to take into account the effects of thermal short-circuiting for CGHEs. Therefore, an analysis of the effects of thermal short-circuiting for CGHEs seems necessary, not only for a correct sizing of these heat exchangers, but also to understand whether techniques to reduce this effect could be useful to improve the thermal performance. Another relevant technical information for the application of CGHEs is the knowledge of the change in performance which occurs if the flow direction is reversed. In fact, a CGHE can operate in two different ways:

a) fluid inlet in the external annular passage;
b) fluid inlet in the internal tube.

The principal aim of this paper is to evaluate the effects of thermal short-circuiting on the performance of CGHEs and to determine how much the performance of a CGHE changes if the flow direction is reversed. A second aim is to evaluate the increase in performance which can be obtained by a slight modification of the cross section of a CGHE. For these purposes, two CGHEs are considered: the first is a CHGE currently used in Italy; the second is a slightly modified version of the first. Results are obtained through finite-element numerical simulations performed by means of the software package COMSOL Multiphysics 3.4 (© Comsol, Inc.).

2. Simulation method

Both CGHEs modelled have length L = 20 m. The real 3-D unsteady conditions of the heat transfer problem are considered. However, on account of the axial symmetry of both the geometry and the initial and boundary conditions, a 2-D axisymmetric model with a cylindrical coordinate system (r, z) is employed, as sketched in Figure 1. Both the CGHE and a portion of the surrounding soil are included in the computational domain; the latter is a cylinder, coaxial with the CGHE, with radius r_0 = 4 m and length L_0 = 24 m. Thus, also a ground layer 4 m thick under the CGHE is modelled.

The first CGHE, which will be called CGHE 1, is a coaxial ground heat exchanger commonly used in Northern Italy, directly driven into the soil. It has an inner tube made either of high density polyethylene, PE-Xa, or of high molecular weight random copolymer polypropylene PP-R80: the external diameter of the inner tube is 32 mm, while the internal diameter thereof is 26.2 mm. The outer tube is made of AISI 304 steel; it has an external diameter of 50 mm and a wall thickness of 2 mm. The second CGHE, which will be called CGHE 2, has a slightly modified geometry, designed to increase the fluid velocity in the outer annular passage and to reduce it in the inner circular tube. In CGHE 2, the inner tube has an external diameter of 40 mm and an internal diameter of 32.6 mm, while the outer AISI 304 steel tube has an external diameter of 54 mm and a thickness of 2 mm. Reference is made to real commercial tubes. Relevant geometrical parameters, material properties and working conditions are listed in Table I.

The mass flow rate considered is 11.5 dm^3/min, with an inlet water temperature of 4°C (winter operation). In these conditions, the water flow is turbulent in the inner tube and laminar in the outer annular passage. Thus, in the inner tube the forced convection heat transfer phenomena are difficult to simulate, while the convection coefficient is not strongly dependent on the thermal boundary condition. On the contrary, in the outer annular passage the laminar forced convection heat transfer can be easily simulated, while the convection coefficients between fluid and walls are strongly dependent on the ratio between the wall heat fluxes [14], which is unknown, non uniform along z and time dependent.

For this reason, the internal flow is not simulated. In the inner tube, the distribution of the fluid bulk temperature T_f along the flow direction z and the heat transfer between fluid and wall are determined by means of the so-called "weak boundary condition" available in COMSOL Multiphysics. In detail, the following energy balance equation for the fluid is coupled with the convective heat transfer boundary condition at $r = r_1$ (internal wall of the inner tube):

$$A_1 \rho_f c_f \frac{\partial T_f}{\partial \tau} = \pm \dot{V} \rho_f c_f \frac{\partial T_f}{\partial z} + h_1 p_1 \left(T_{r1} - T_f \right) \quad . \qquad (4)$$

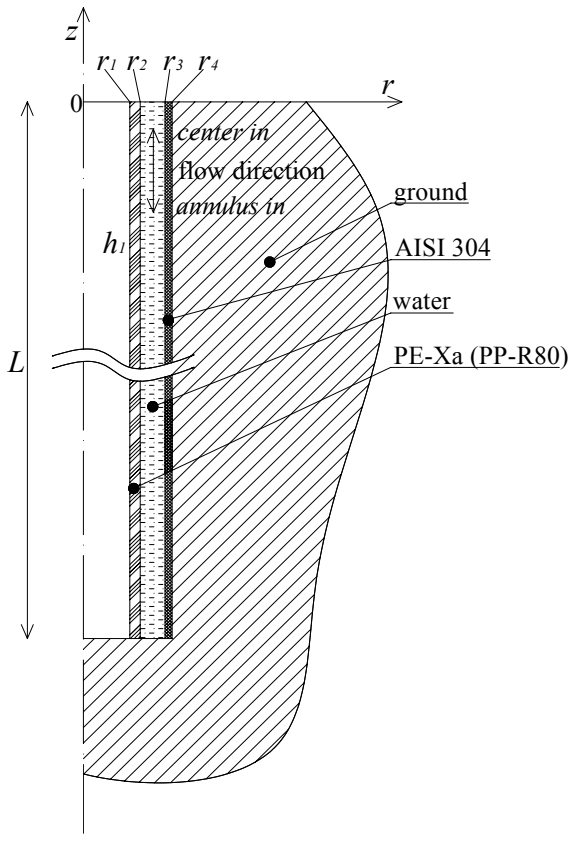

Fig. 1. Sketch of the computational domain.

TABLE I. –Values of relevant geometrical parameters, thermal properties and working conditions.

SYMBOL	VALUE	QUANTITY
Geometrical data of CGHE 1		
r_1	13.1	Internal radius of inner tube [mm]
r_2	16	External radius of inner tube [mm]
r_3	23	Internal radius of outer tube [mm]
r_4	25	External radius of outer tube [mm]
L	20	Length [m]
Geometrical data of CGHE 2		
r_1	16.3	Internal radius of inner tube [mm]
r_2	20	External radius of inner tube [mm]
r_3	25	Internal radius of outer tube [mm]
r_4	27	External radius of outer tube [mm]
L	20	Length [m]
Thermal properties of AISI304 steel		
c_a	500	Specific heat capacity [J/(kg K)]
k_a	15	Thermal conductivity [W/(m K)]
ρ_a	7910	Density [kg/m^3]
Thermal properties of high density polyethylene PE-Xa		
c_1	2300	Specific heat capacity [J/(kg K)]
k_1	0.35	Thermal conductivity [W/(m K)]
ρ_1	940	Density [kg/m^3]
Thermal properties of high molecular weight random copolymer polypropylene PP-R80		
c_2	2000	Specific heat capacity [J/(kg K)]
k_2	0.24	Thermal conductivity [W/(m K)]
ρ_2	900	Density [kg/m^3]
Thermal and rheological properties of water at T = 4.3 °C		
c_{pf}	4207	Specific heat capacity at constant pressure [J/(kg K)]
k_f	0.5692	Thermal conductivity [W/(m K)]
ρ_f	999.97	Density [kg/m^3]
μ_f	1.552	Dynamic viscosity [mPa s]
Thermal properties of ground		
$(\rho c)_g$	2000	Heat capacity per unit volume [J/(m^3 K)]
k_{g1}	1.4	Thermal conductivity 1 [W/(m K)]
k_{g2}	2.8	Thermal conductivity 2 [W/(m K)]
Working conditions		
T_{in}	4	Water inlet temperature [°C]
T_s	4	Ground surface temperature [°C]
T_g	14	Undisturbed ground temperature [°C]
$\dot{V}$	11.5	Water flow rate [dm^3/min]

In Eq. (4): $A_1 = \pi r_1^2$ is the inner tube cross-section area, τ is time, $p_1 = 2\pi r_1$ is the internal wall perimeter per unit length, T_{r1} is the internal wall temperature, h_1 is the convection heat transfer coefficient; the sign + in the first term of the right hand side holds for downward flow (water inlet in the inner tube), while the sign – in the same term holds for upward flow (water inlet in the annular passage). The value to be assigned to the internal Nusselt number and, therefore, to h_1 is determined by means of the Churchill correlation [15]. One obtains $h_1 \approx$ 1520 W/(m^2 K) for CGHE 1 (Reynolds number Re = 6001) and $h_1 \approx$ 968 W/(m^2 K) for CGHE 2 (Reynolds number Re = 4823).

In the annular passage, the forced convection flow is considered as fully developed, because the length of the duct is three orders of magnitude higher than the duct mean diameter. The laminar fluid velocity profile $U(r)$ in the annular duct, which has internal radius r_2 and external radius r_3, is given by [16]

$$U(r) = U_m \frac{2\left\{\left[\left(\frac{r_2}{r_3}\right)^2 - 1\right]\ln\frac{r}{r_3} - \left[\left(\frac{r}{r_3}\right)^2 - 1\right]\ln\frac{r_2}{r_3}\right\}}{1 - \left(\frac{r_2}{r_3}\right)^2 + \left[1 + \left(\frac{r_2}{r_3}\right)^2\right]\ln\frac{r_2}{r_3}} \quad , \quad (5)$$

where $U_m = \dot{V} \Big/ \left[\pi\left(r_3^2 - r_2^2\right)\right]$ is the mean fluid velocity in the duct, which is positive for upward flow (water inlet in the inner tube) and negative for downward flow (water inlet in the annular passage). The convection heat transfer in the annular duct is simulated with the velocity distribution given by Eq. (5).

The differential equations to be solved are

$$\rho_f c_{pf}\left[\frac{\partial T}{\partial \tau} + (\mathbf{U}\cdot\nabla)T\right] = k_f \nabla^2 T \quad , \quad (6)$$

with $\mathbf{U} = (0, U)$ and $U = U(r)$ given by Eq. (5), in the annular duct;

$$\rho c \frac{\partial T}{\partial \tau} = k \nabla^2 T \quad , \quad (7)$$

with the thermal properties of the material present in the subdomain considered, for all the other subdomains.

As initial condition, a depth-dependent temperature distribution in the soil $T_0(z)$ is considered, which accounts both for the steep temperature gradient near the ground surface and for the geothermal gradient. The following expression of $T_0(z)$ has been assumed,

$$T_0(z) = T_g + (T_s - T_g)e^z + H(-10 - z)\cdot TG\cdot(-10 - z) \quad , \quad (8)$$

where T_g is the undisturbed ground temperature, H is the Heaviside unit step function, $TG = 0.03$ °C/m is the geothermal gradient and $-24\ \text{m} \le z \le 0$. The same initial condition is adopted for the CGHE, which is assumed to be in thermal equilibrium with the ground. For $t > 0$, the inlet water temperature T_{in} is prescribed and constant, as well as the surface ground temperature T_s. The external vertical and bottom surfaces of the modelled ground are kept at the constant temperature $T_0(z)$.

Clearly, the continuity conditions are imposed at the interfaces between different materials, while the "outflow pressure" condition is imposed at the fluid outlet.

In order to grant that the results are independent of the domain extension, most simulations have been repeated by replacing the boundary condition $T = T_0(z)$, at the external vertical and bottom surfaces, with the boundary condition of adiabatic surfaces. The check has always given the same results as those obtained with the first boundary condition.

A period of five days of operation, with fixed values of the water inlet temperature and of the volume flow rate, is considered for each CGHE. Clearly, the temperature changes are steeper during the first minutes and become much slower as time goes by. Therefore the following time steps are adopted in computations: 1s for $0 < \tau < 60\,\text{s}$, 5s for $60\,\text{s} < \tau < 600\,\text{s}$, 60s for $600\,\text{s} < \tau < 3600\,\text{s}$, 600s for $3600\,\text{s} < \tau < 43200\,\text{s}$, 7200s for $43200\,\text{s} < \tau < 432000\,\text{s}$. The thermal power $\dot{Q}$

exchanged between the CGHE and the surrounding soil, as a function of time, is determined as

$$\dot{Q} = \int_S k_g \, \nabla T \cdot \mathbf{n} \, dS \quad , \tag{9}$$

where ∇T is evaluated in the ground, S is the boundary surface of the CGHE and **n** is the outward unit normal.

3. Results

In order to point out the effects of flow direction on the performance of a CGHE, two directions of the water flow in the tubes have been considered: water inlet in the outer annular passage, which will be denoted by *annulus-in*, water inlet in the inner tube, which will be denoted by *center-in*. Moreover, to point out the effects of thermal short-circuiting, three different thermal conductivities of the material which forms the inner tube have been considered: the thermal conductivity of polyethylene PE-Xa, k_1 = 0.35 W/(mK); the thermal conductivity of polypropylene PP–R80, k_2 = 0.24 W/(mK); a nearly vanishing thermal conductivity k = 0.0001 W/(mK), to simulate an adiabatic wall of the inner tube.

Finally, to investigate the influence of the thermal conductivity of the ground on the effects of flow direction and of thermal short-circuiting, two different kinds of ground have been considered: GROUND 1, with a low thermal conductivity, k_{g1} = 1.4 W/(mK); GROUND 2, with a high thermal conductivity, k_{g2} = 2.8 W/(mK). A standard value of the heat capacity per unit volume, 2 MJ/(m^{3}K), has been considered for both grounds. All the calculations have been performed for two CGHEs: CGHE 1 and CGHE 2, with different geometrical features, summarized in Table I.

In order to ensure the grid independence of results, three different mapped meshes have been tested: Mesh 1, with about 13300 elements; Mesh 2, with about 22000 elements; Mesh 3, with about 29000 elements. A comparison of the results obtained with the different meshes is illustrated in Table II, where the values of the energy collected by CGHE 1 in GROUND 1 are reported for some time intervals after the start-up, in the *annulus-in* configuration and with inner tube made of PE-Xa.

The results show that the discrepancies between Mesh 2 and Mesh 3 are very small. Therefore, Mesh 2 has been adopted for all the computations reported in the following. A sketch of Mesh 2 is represented in Figure 2.

The main parameter analyzed is the energy collected by a CGHE as a function of time. The results for this parameter, for some selected time intervals, are reported in Tables III and IV, for all the considered cases.

TABLE II. – Energy collected by CGHE 1, calculated using Mesh 1, Mesh 2 and Mesh 3.

Energy [MJ] CGHE 1, GROUND 1, PE-Xa, *annulus-in*			
Time	***Mesh 1*** ***(13263 elements)***	***Mesh 2*** ***(22185 elements)***	***Mesh 3*** ***(29005 elements)***
300 s	0.4999	0.5042	0.5059
900 s	1.396	1.404	1.407
3600 s	4.269	4.279	4.278
6 h	17.54	17.53	17.57
24 h	54.25	54.23	54.31
5 days	210.9	211.2	211.4

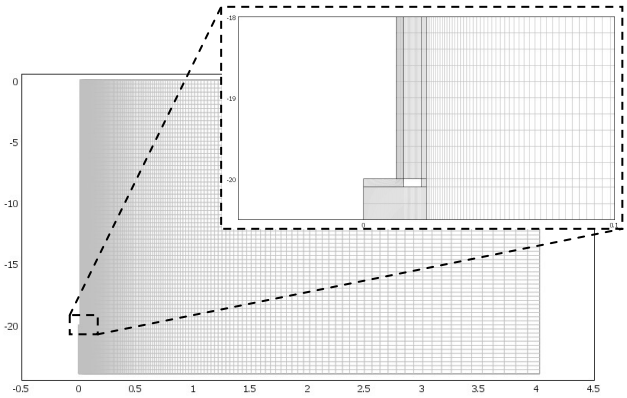

Fig. 2. Sketch of Mesh 2.

TABLE III. – Energy collected in different time periods for CGHE 1.

	Energy [MJ] CGHE 1 – GROUND 1					
	Annulus-in			*Center-in*		
Time	***PE-Xa***	***PP-R80***	***adiabatic***	***PE-Xa***	***PP-R80***	***adiabatic***
300 s	0.504	0.510	0.519	0.345	0.355	0.391
900 s	1.40	1.41	1.42	1.28	1.28	1.32
3600 s	4.28	4.29	4.31	4.15	4.20	4.19
6 h	17.5	17.5	17.6	17.4	17.4	17.4
24 h	54.2	54.3	54.5	53.9	53.9	54.1
5 days	211	211	212	210	210	211

	Energy [MJ] CGHE 1 – GROUND 2					
	Annulus-in			*Center-in*		
Time	***PE-Xa***	***PP-R80***	***adiabatic***	***PE-Xa***	***PP-R80***	***adiabatic***
300 s	0.618	0.625	0.636	0.415	0.427	0.471
900 s	1.80	1.81	1.83	1.61	1.62	1.67
3600 s	5.94	5.95	6.00	5.71	5.77	5.78
6 h	25.0	26.5	26.7	26.0	26.1	26.2
24 h	86.1	86.3	86.9	85.1	85.2	85.5
5 days	349	349	352	345	345	347

TABLE IV. – Energy collected in different time periods for CGHE 2.

	Energy [MJ] CGHE 2 – GROUND 1					
	Annulus-in			*Center-in*		
Time	***PE-Xa***	***PP-R80***	***adiabatic***	***PE-Xa***	***PP-R80***	***adiabatic***
300 s	0.601	0.608	0.628	0.349	0.364	0.415
900 s	1.60	1.61	1.64	1.40	1.42	1.47
3600 s	4.71	4.75	4.76	4.56	4.59	4.60
6 h	18.8	18.8	18.9	18.6	18.6	18.7
24 h	57.3	57.4	57.7	56.9	57.1	57.2
5 days	221	221	222	219	220	221

	Energy [MJ] CGHE 2 – GROUND 2					
	Annulus-in			*Center-in*		
Time	***PE-Xa***	***PP-R80***	***adiabatic***	***PE-Xa***	***PP-R80***	***adiabatic***
300 s	0.744	0.751	0.779	0.419	0.438	0.502
900 s	2.09	2.10	2.15	1.79	1.82	1.89
3600 s	6.68	6.66	6.73	6.38	6.42	6.49
6 h	28.8	28.8	29.0	28.3	28.4	28.8
24 h	92.2	92.4	92.9	91.1	91.4	92.0
5 days	370	370	372	365	366	368

TABLE V. – Percent difference between energy collected with flow direction *center-in* and energy collected with flow direction *annulus-in*.

CGHE 1 – GROUND 1			
Time	***PE-Xa***	***PP-R80***	***adiabatic***
300 s	-31.59	-30.38	-24.60
900 s	-9.08	-9.18	-7.27
3600 s	-2.91	-2.21	-2.63
6 h	-0.93	-0.69	-1.10
24 h	-0.68	-0.61	-0.81
5 days	-0.66	-0.67	-0.26

CGHE 1 – GROUND 2			
Time	***PE-Xa***	***PP-R80***	***adiabatic***
300 s	-32.93	-31.71	-25.92
900 s	-10.53	-10.49	-8.64
3600 s	-3.78	-2.96	-3.53
6 h	-1.70	-1.53	-1.98
24 h	-1.17	-1.36	-1.54
5 days	-1.28	-1.25	-1.32

CGHE 2 – GROUND 1			
Time	***PE-Xa***	***PP-R80***	***adiabatic***
300 s	-41.92	-40.13	-33.99
900 s	-12.09	-11.85	-10.47
3600 s	-3.23	-3.33	-3.40
6 h	-1.14	-1.05	-1.22
24 h	-0.69	-0.56	-0.92
5 days	-0.58	-0.71	-0.42

CGHE 2 – GROUND 2			
Time	***PE-Xa***	***PP-R80***	***adiabatic***
300 s	-43.72	-41.71	-35.53
900 s	-14.27	-13.36	-12.09
3600 s	-4.47	-3.73	-3.67
6 h	-1.75	-1.48	-0.98
24 h	-1.25	-1.05	-0.96
5 days	-1.18	-1.13	-1.01

A. Effect of flow direction

The effect of flow direction on the thermal performance of CGHEs is illustrated in Table V, where the percent difference between the energy collected with the flow direction *center-in* and that collected with the flow direction *annulus-in* is reported, respectively for CGHE 1 in GROUND 1, CGHE 1 in GROUND 2, CGHE 2 in GROUND 1 and CGHE 2 in GROUND 2. In all cases, the results are negative, *i.e.*, the *annulus-in* flow direction is preferable to the *center-in* flow direction. The effect is important in the first 5 minutes, where it can be higher than 40%, remains important for about 15 minutes (8–13%), then decreases and becomes lower than 2% after 6 hours. The effect is more important in the higher conductivity ground and for the higher efficiency CGHE.
The reason for the higher performance of a CGHE which operates with the *annulus-in* flow direction, in the first minutes, is as follows. In the *annulus-in* configuration, the cold inlet water flows directly at contact with the AISI external tube, starting from the first instants of operation. On the contrary, if the *center-in* flow direction is adopted, the cold inlet water must first circulate along the whole inner tube before reaching the contact with the outer AISI wall of the external annular passage, at the bottom of the CGHE.

B. Effect of thermal short-circuiting

The effect of thermal short-circuiting on the performance of CGHEs is illustrated in Table VI, where the percent energy loss due to short-circuiting (with respect to the ideal case of adiabatic inner wall) is reported, respectively for CGHE 1 in GROUND 1, CGHE 1 in GROUND 2, CGHE 2 in GROUND 1 and CGHE 2 in GROUND 2.
As is shown by the results reported in Table VI, the effect of thermal short-circuiting on the performance of CGHEs

is not very important, especially for the recommendable flow direction, *annulus-in*, *i.e.*, with fluid inlet in the outer annular passage. For this flow configuration, the energy loss is higher than 4% only for CGHE 2 (the more efficient one) for a time interval of 5 minutes after the start-up of the CGHE. Then, it decreases rapidly and becomes lower than 1% for time intervals longer than 1 hour. For the *center-in* flow direction, *i.e.*, with fluid inlet in the central tube, the effect of thermal short-circuiting can be very important during the first 5 minutes, where it can exceed 12%. Indeed, the first 5 minutes are a very critical time interval for the operation of a CGHE in the *center-in* configuration. In fact, the cold inlet water reaches the contact with the AISI external wall with a time delay of about 1 minute. Therefore, during the first minutes, the heat transfer between the external wall of the CGHE and the ground is not efficient and, as a consequence, the short-circuiting heat transfer between the coaxial tubes plays an important role.

The effects of flow direction and of thermal short-circuiting are illustrated in Figure 3, where the power exchanged with the ground is plotted versus time, for CGHE 2 in GROUND 2, for both flow configurations, with internal tube in PE-Xa and with an ideal adiabatic internal tube. For the *center-in* flow configuration, the power is negative for about 90 s. This phenomenon is due to the fact that, while the cold inlet water fills the inner tube, the warm water present in the bulk of the outer tube flows out and heats the cold soil layers which are placed close to the ground surface.

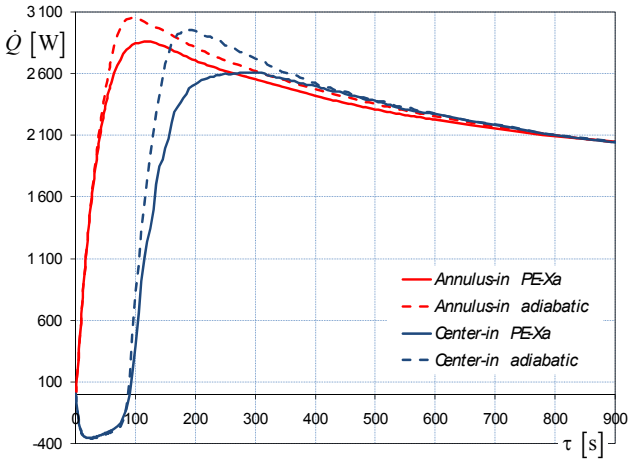

Fig. 3. Power collected by CGHE 2 in GROUND 2, with internal tube in PE-Xa and with adiabatic internal tube.

C. Increase in thermal performance obtained by CGHE 2

The basic idea which led us to design CGHE 2 is the following. In CGHE 1, the major part of the distributed pressure drop due to viscous friction occurs in the inner circular tube, where the flow is turbulent with Re = 6001. On the contrary, it is better to use the work of the pump to enhance the mean velocity of water in the outer annular passage, where heat transfer with the AISI external wall and thus with the ground occurs. Therefore, the inner tube has been replaced by the next larger one available on the market. In order to keep the total pressure drop nearly unchanged, it has been necessary to replace also the outer AISI tube by the next larger one available on the market. In this way, a 8% increase of the external area of the CGHE has been produced; a part of the improvement of the thermal performance is due to this increase, which has been necessary to make reference to commercial tubes.

TABLE VI. – Percent energy loss due to thermal short-circuiting.

CGHE 1 – GROUND 1				
	Annulus-in		*Center-in*	
Time	***PE-Xa***	***PP-R80***	***PE-Xa***	***PP-R80***
300 s	2.86	1.76	11.87	9.30
900 s	1.35	0.85	3.27	2.90
3600 s	0.67	0.39	0.95	0.00
6 h	0.57	0.46	0.41	0.06
24 h	0.55	0.47	0.42	0.27
5 days	0.35	0.28	0.76	0.68

CGHE 1 – GROUND 2				
	Annulus-in		*Center-in*	
Time	***PE-Xa***	***PP-R80***	***PE-Xa***	***PP-R80***
300 s	2.88	1.86	12.06	9.52
900 s	1.54	1.02	3.58	3.03
3600 s	0.97	0.84	1.22	0.25
6 h	0.86	0.71	0.58	0.26
24 h	0.87	0.64	0.50	0.46
5 days	0.77	0.72	0.73	0.65

CGHE 2 – GROUND 1				
	Annulus-in		*Center-in*	
Time	***PE-Xa***	***PP-R80***	***PE-Xa***	***PP-R80***
300 s	4.30	3.29	15.80	12.28
900 s	2.63	1.92	4.38	3.42
3600 s	1.12	0.26	0.94	0.19
6 h	0.81	0.52	0.72	0.35
24 h	0.67	0.50	0.44	0.14
5 days	0.49	0.30	0.64	0.59

CGHE 2 – GROUND 2				
	Annulus-in		*Center-in*	
Time	***PE-Xa***	***PP-R80***	***PE-Xa***	***PP-R80***
300 s	4.47	3.53	16.60	12.78
900 s	2.50	2.21	4.92	3.63
3600 s	0.85	1.03	1.68	1.09
6 h	0.77	0.67	1.53	1.18
24 h	0.68	0.54	0.97	0.64
5 days	0.71	0.57	0.88	0.70

The percent difference between the energy collected by CGHE 2 and that collected by CGHE 1 is illustrated in Table VII, with reference to the recommended flow direction, namely the *annulus-in* configuration.

The results reported in Table VII show that the percent difference between the energy collected by CGHE 2 and that collected by CGHE 1 is significant, especially for short time intervals after the start-up of the CHGE, and is greater for the higher conductivity ground. In GROUND 2, it is about 20% for the first 5 minutes, 15-16% for the first 15 minutes, about 12% for the first hour and about 6% for a time interval of 5 days.

TABLE VII. – Percent difference between the energy collected by CGHE 2 and that collected by CGHE 1, with *annulus-in* flow direction.

	GROUND 1		*GROUND 2*	
Time	***PE-Xa***	***PP-R80***	***PE-Xa***	***PP-R80***
300 s	19.25	19.17	20.40	20.32
900 s	13.78	14.04	15.92	15.64
3600 s	10.07	10.72	12.44	12.08
6 h	7.18	7.37	8.83	8.77
24 h	5.69	5.79	7.10	7.00
5 days	4.50	4.62	5.80	5.89

4. Conclusions

The effects of flow direction and of thermal short-circuiting on the performance of coaxial ground heat exchangers have been studied numerically, by finite-element simulations performed through the software package COMSOL Multiphysics 3.4. The real 2-D axisymmetric unsteady heat conduction and convection problem has been considered.

Two Coaxial Ground Heat Exchangers (CGHEs) with a length of 20 m have been examined: the first is a CGHE commonly employed in Northern Italy; the second is an improvement of the first, proposed here. The distribution of the fluid bulk temperature in the inner circular tube has been determined by means of the "weak boundary form" boundary condition available in COMSOL Multiphysics. The laminar convective heat transfer in the outer annular passage has been simulated directly, by assuming a fully developed velocity profile in the whole duct. The computational domain has included the surrounding soil in a radius of 4 m, as well as a 4 m thick soil layer beneath the CHGE. Two different values of the ground thermal conductivity, as well as two different materials for the inner tube wall have been considered. The results lead to the following conclusions.

The *annulus-in* flow direction (fluid inlet in the outer annular passage) is more efficient than the *center-in* flow direction (fluid inlet in the inner circular tube). The effect is important in the first 5 minutes, where it can be higher than 40%, then decreases and becomes lower than 2% after 6 hours. The effect of short-circuiting is not very important, if the *annulus-in* flow direction is employed: it has values higher than 4% only for the more efficient CGHE for a time interval of 5 minutes; then, it decreases rapidly and becomes lower than 1% for time intervals longer than 1 hour. For the *center-in* flow direction, the effect of thermal short-circuiting can be very important during the first 5 minutes, where it can exceed 12%.

The enhancement of the thermal performance obtained by means of the new designed CHGE is significant, especially for short time intervals and for high conductivity ground.

References

[1] 2007 ASHRAE Handbook – HVAC Applications, Ch. 32.

[2] R.L. Ingersoll and A.C. Zobel, Heat conduction with engineering and geological applications, McGraw-Hill, New York (1954).

[3] S.P. Kavanaugh, Simulation and experimental verification of a vertical ground-coupled heat pump system, Ph.D. dissertation, Oklahoma State University, Stillwater, 1985.

[4] S. Gehlin and B. Nordell, "Determining Undistrurbed Ground Temperature for Thermal Response Tests", ASHRAE Transactions, Vol. 109, 151-156 (2003).

[5] P. Roth *et al*., "First in situ determination of ground and borehole thermal properties in Latin America", Renewable Energy, Vol. 29, pp. 1947-1963 (2004).

[6] S. Signorelli *et al.*, "Numerical evaluation of thermal response tests", Geothermics, Vol. 36, 141-166 (2007).

[7] C. Yavuzturk, J.D. Spitler and S.J. Rees, "A Transient Two-Dimensional Finite Volume Model for the Simulation of Vertical U-tube Ground Heat Exchangers", ASHRAE Transactions, Vol. 105 (2), pp. 465-474 (1999).

[8] W.A. Austin, C. Yavuzturk and J.D. Spitler, "Development of an In-Situ System and Analysis Procedure for Measuring Ground Thermal Properties", ASHRAE Transactions, Vol. 106 (1), pp. 365-379 (2000).

[9] S. Gehlin and G. Hellström, "Comparison of four models for thermal response test evaluation", ASHRAE Transactions, Vol. 109, pp. 131-142 (2003).

[10] H.S. Carlslaw and J.C. Jaeger, Conduction of Heat in Solids, Oxford University Press, Oxford (1959).

[11] H. Zeng, N. Diao and Z. Fang, "Heat transfer analysis of boreholes in vertical ground heat exchangers", Int. J. Heat Mass Transfer, Vol. 46, pp. 4467−4481 (2003).

[12] L. Lamarche and B. Beauchamp, "New solutions for the short-term analysis of geothermal vertical boreholes", Int. J. Heat Mass Transfer, Vol. 50, pp. 1408-1419 (2007).

[13] D. Marcotte and P. Pasquier, "On the estimation of thermal resistance in borehole thermal conductivity test", Renewable Energy, Vol. 33, pp. 2407-2415 (2008).

[14] S. Kakac and Y. Yener, Convective heat transfer, Second Edition, CRC (1995), Section 6-15, pp. 172-179.

[15] S. W. Churchill, "Comprehensive correlating equations for heat, mass and momentum transfer in fully developed flow in smooth tubes", Ind. Eng. Chem. Fundam., Vol. 16, pp. 109-116 (1977).

[16] E. Zanchini, "Mixed convection with variable viscosity in a vertical annulus with uniform wall temperatures", Int. J. Heat Mass Transfer, Vol. 51, pp. 30-40 (2008).